Effect of Misalignment on the Performance of Planetary Gear Journal Bearings

by

D. Vijayaraghavan[1]
Dept. of Mechanical Engineering
The University of Toledo
Toledo, Ohio 43606

and

D. E. Brewe
US Army Vehicle Technology Directorate
NASA Glenn Research Center
Cleveland, Ohio 44135

ABSTRACT

Planetary gear systems are an efficient means of achieving higher reduction ratios with minimum space and weight. They are used in helicopter, aerospace, automobile and many industrial applications. One of the major operating problems in these bearings is misalignment, mainly, due to the operating variables and differential elastic responses of the individual components of the gear train. The effects of axial and twisting misalignment, on the performance of an axial grooved journal bearing of a planetary gear is the focus of this investigation. A comprehensive THD model with heat transfer within the fluid film and heat dissipation to the ambient through the journal and bush, is utilized. Cavitation modeling with regard to thermal effects and mass conservation are carefully considered. A non-dimensional analysis is performed to provide generality for the results. For varying degrees of misalignment and transmitted torque, variations in bearing performance parameters such as film thickness, pressure, side leakage, and temperature are presented.

---

[1]   **Resident at NASA/LeRC, Cleveland, Ohio**

INTRODUCTION

Planetary gear systems are widely used in helicopter transmissions, aircraft turbine engine reduction gears, automotive automatic transmissions and many industrial applications. Because of multiple load paths of planetary gearing, the horsepower transmitted is divided between several planet meshes. Thus the gear size can be reduced significantly compared to parallel shaft designs. In addition, planetary stages can also be linked together efficiently to achieve high reduction ratios in a minimum space. Because of their compactness, planetary gear systems offer significant envelope and weight savings. They have reduced noise, vibration, and improved efficiency due to smaller, stiffer components. Since the input and output shaft axes are concentric, they are effective in transmitting torque. Therefore, there is a trend toward increased utilization of planetary gears for industrial applications.

High-speed planetary gear systems will have significant dynamic loading and high heat generation. Hence, they need jet lubrication and associated cooling systems. Hydrodynamic journal bearings are a must for critical applications that necessitate high reliability and long life when the torque loading is very large and when downtime cost is significantly more than initial cost. Further, the types of failure in journal bearings are less catastrophic and easier to detect [Lynwander, (1983)]. Since, each shaft must be radially and axially located by the bearings and the power loss due to friction and churning is to be kept at a minimum to improve the efficiency, proper bearing design is at least as important to the operation of the system as is the design of the gears.

One of the major operating problems of these bearings is misalignment. The individual components of the gear train undergo a twist, under the torque load being transmitted, depending upon their rotational stiffness. The differential twists between the planet gear and the journal results in misalignment. The misalignment can also result from asymmetry in applied load, thermal distortion, manufacturing error, and/or improper installation. Since these units are compact and the applied loads are large, these bearings can have large length to diameter ratios, making it susceptible for misalignment. Even if it were possible to perfectly align the equipment for a given operating point, because load, speed or ambient conditions vary, alignment can change. Das and Gupta (1980), in their analysis of determining misalignment in the journal bearing of a planetary gear system, highlight the adverse effects and determined that the carrier stiffness plays a major part in controlling the misalignment. The misalignment could be purely axial or purely twisting or any combination of these. Hence, studying the performance of fluid film bearings with misalignment is an important step toward a reliable design.

McKee and McKee (1932) were one of the first to point out that, in the case of eccentric loading, the maximum film pressure will be off the axial center of the bearing in the same direction as the shift in load. DuBois et al (1951, 1957) conducted detailed experiments to determine the effect of misalignment on the performance of journal bearings. Smalley and McCallion (1966) theoretically determined the effect of misalignment for an ungrooved journal bearing. Pinkus and Bupara (1979) performed detailed analysis on an axially grooved bearing and presented numerous charts and tables. Braun et al (1983) included the temperature effects for a finite journal bearing with spatial tilt. Vijayaraghavan and Keith (1990) analyzed the misaligned journal bearing performance by including the cavitation and starvation effects.

Lubricant viscosity strongly depends on the temperature and pressure values. It is common, in the operation of journal bearings, for the viscosity within the film to be different by a factor of 50. In addition, consideration of cavitation effects in a thermo-hydrodynamic analysis is very important in order to correctly predict the flow, viscous dissipation and heat flow through the entire bearing clearance as well as to determine the side leakage, power loss and heat transport to the bearing shell and journal. Therefore, a model which correctly includes the cavitation and thermal effects in the analysis would simulate the operating conditions better and provide improved predictive capability. The surveys by Khonsari (1987) and Pinkus (1990) highlight the attention given to thermal effects and all the advances that have been made thus far. Paranjpe and Han (1994?) have analyzed the performance of statically and dynamically loaded journal bearings, typically used in automotive applications, using a cavitation algorithm and the energy equation. Based on the JFO (Jakobsson-Floberg-Olsson) cavitation model, Elrod and Vijayaraghavan (1995) developed an efficient THD numerical procedure to analyze journal bearing performance. The model incorporates cavitation effects and expresses the distribution of fluid properties across the film thickness using collocated polynomials. However, the model does not account for differential thermal expansion between the shaft and bearing, which can have a significant effect. Gethin (1985) measured higher load capacity, higher maximum temperature, and a reduction in side-leakage as a result of shaft thermal expansion and local bush deformation. Khonsari and Wang (1991) confirmed the same effect without shaft deformation. Ferron, et al. (1983) show that for a given load the calculated eccentricity can be slightly less than experiments dictate under conditions of differential dilatation. Thus the calculations in this investigation will have a tendency to predict higher film thickness, lower maximum temperatures, decreased load capacity, and greater side-leakage. By accounting for an effective decrease in radial clearance and eccentricity caused by the differential thermal expansion, Vijayaraghavan (1996) showed the predictions made by the present theory were

3

in excellent agreement with the experiments by Ferron, et al. (1983). While this would affect the overall accuracy of the calculations, it would not have an effect on the stated trends and/or the conclusions of this study. Albeit, with the inclusion of conduction through the bearing shell and journal, this procedure constitutes a highly comprehensive THD model.

For this study an epicyclic planetary gear system is considered (See Figure 1). In this arrangement, the input is through the sun gear and output is from the planet gears connected to a carrier which rotates about the center of the system. The ring gear is stationary. Hence, the planet gear rotates about the carrier pin as well as revolves
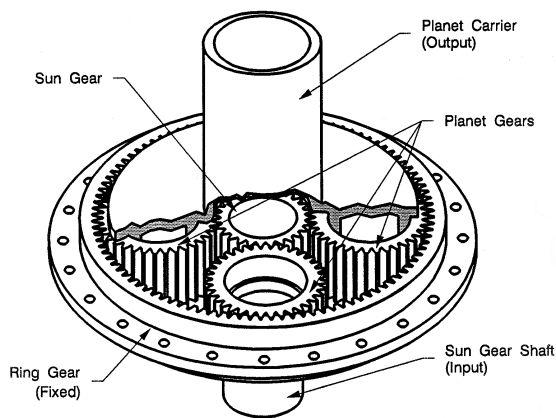

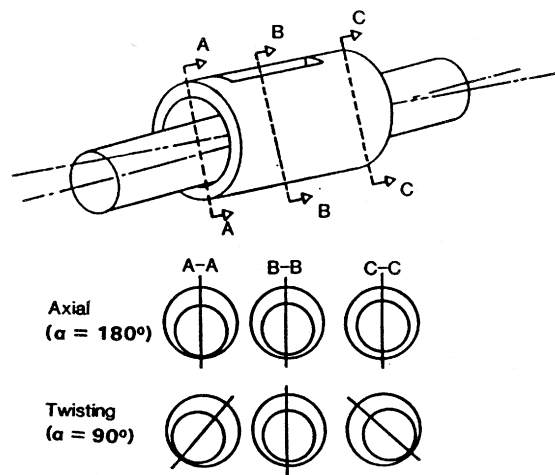**Figure 1 Planetary Gear System**

Figure 2 Axial and Twisting Misalignment

around the sun gear. The bore of the planet gear (rotating bearing shell) and the carrier pin (a stationary journal) make up the journal bearing. Pressurized lubricant is supplied from the hollow journal/carrier pin via an orifice to an axial groove on the journal/carrier pin outer surface. The radial forces on the bearing due to the rotation of the planet gear is assumed to be constant and the tangential force applied on the bearing is varied depending upon the amount of torque load being transmitted. This results in varying magnitude and orientation of the load vector. The misalignment (Figure 2), either axial (vertical) or twisting (horizontal), with varying degrees of misalignment are considered.[2] The comprehensive THD model (described above) is used to conduct the study.

---

[2] Axial misalignment is defined as the condition in which a couple is applied to the bearing/planet in a plane containing the line of action of the central load and the axis of the journal. Twisting misalignment is defined as the condition in which a couple is applied to the bearing/planet in a plane perpendicular to the line of action of the main load.

Roelands' (1966) model of the viscosity-temperature-pressure relationship is used to determine the viscosity profile of the lubricant. The approach taken by Pinkus and Bupara (1979) and Vijayaraghavan and Keith (1990) to characterize the general misalignment conditions and the representation of the film thickness is adopted here. To enable parametric comparisons, a non-dimensional analysis is performed. The study seeks to portray how varying degrees of misalignment, D_m, ranging from 0 (perfect alignment) to 0.8 (severe misalignment) can affect heat generation and bearing performance. The effects of the tangential reactionary force to the sun gear/ring gear engagement with the planet gear are included.

GOVERNING EQUATIONS

For a Newtonian fluid in laminar flow, the governing equations and the numerical procedure for a thermo-hydrodynamic analysis of cavitating bearings, using Legendre polynomials collocated at Lobatto points, have been developed by Elrod (1991) and Vijayaraghavan (1996). Basically, fluidity, ξ, which is the reciprocal of viscosity, η, is used as a dependent variable and expressed as a series of Legendre polynomials at the chosen Lobatto points across the film thickness. The hydrodynamic equation in non-dimensional form can be written as,

$$12\frac{\partial(\theta\bar{h})}{\partial\tau} \;+\; 6\vec{V}^{+}\cdot\vec{\nabla}\left(\theta\bar{h}\right) \;-\; 6\vec{V}^{-}\cdot\vec{\nabla}\left(\frac{\underline{\xi}_1}{\underline{\xi}_o}\theta\bar{h}\right) = \vec{\nabla}\cdot\left(\bar{\xi}_p\,\bar{h}^{3}\,g\,\bar{\beta}\,\vec{\nabla}\,\theta\right) \tag{1}$$

where

$$\theta \;=\; \begin{cases} \rho/\rho_c \geq 1 & \textit{in a full film region} \\ < 1 & \textit{partial film content in cavitated region} \end{cases}$$

$$g \quad = \quad \begin{cases} 1 \; if \; \theta \geq 1 \\ 0 \; if \; \theta < 1 \end{cases}$$

$$\bar{p} = \bar{p}_c + g(\theta - 1)$$

$$\bar{\xi}_p = \underline{\xi}_0 + 0.4\underline{\xi}_2 - \left(\underline{\xi}_1^2 \Big/ 3\underline{\xi}_0 \right)$$

$$\vec{V}^+ = \left(\vec{V}_U + \vec{V}_L \right) \Big/ U_L \qquad \vec{V}^- = \left(\vec{V}_U - \vec{V}_L \right) \Big/ U_L$$

As per JFO theory, the fluid in the cavitated region is confined within striations of varying width (see Fig. 3), extending between film rupture and reformation boundaries and between bounding surfaces. Our interest in
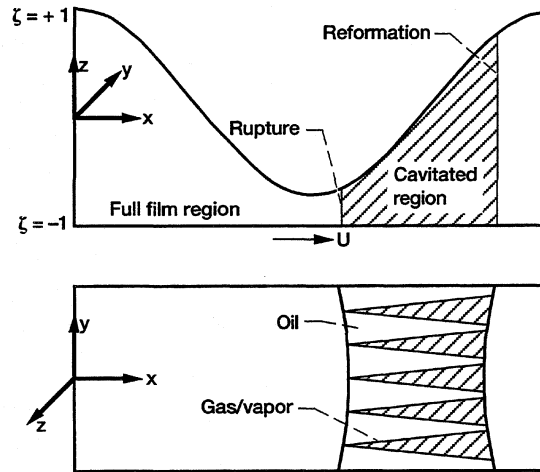

**Figure 3 Schematic Diagram of a Cavitating
Bearing with Striated Flow**

determining the temperature profile in this region is only for the fluid. Hence, the energy equation in the cavitated region is for striations only. The thermal energy equation, applicable for the full film, as well as, for the striations in the cavitated region, is written in non-dimensional form as,

6

$$\partial \overline{T} \Big/ \partial \tau + \vec{V} \cdot \vec{\nabla} \overline{T} + \left(D\zeta \Big/ D\tau \right) \partial \overline{T} \Big/ \partial \zeta = \frac{4}{P e_f \overline{h}^2} \partial^2 \overline{T} \Big/ \partial \overline{T}^2 + \frac{4\Phi}{\overline{h}^2 \Phi^*}$$

(2)

where

$$D\zeta \Big/ D\tau = -\frac{1}{\overline{h}} \left[(1 + \zeta) \frac{\partial \overline{h}}{\partial \tau} + \vec{\nabla} \cdot \overline{h} \int_{-1}^{\zeta} \vec{V} d\zeta \right]$$

$$\Phi = \frac{\left[\left(\frac{\partial u}{\partial \zeta} \right)^2 + \left(\frac{\partial v}{\partial \zeta} \right)^2 \right]}{\overline{\xi}}$$

Note that Φ^* is defined in the nomenclature as a non-dimensional parameter and is a constant coefficient (see Table I) to the viscous dissipation term for this investigation. In the cavitated region, the striation width will be very small compared to its length. Using short bearing theory approximation, Elrod and Vijayaraghavan (1995) developed a procedure to evaluate the Lagrangian derivative, $D\zeta/D\tau$, for the striations and handling reverse flow at the reformation interface.

Roelands (1966) compiled and investigated extensive experimental data available for a wide range of lubricants over a wide range of temperatures and pressures and proposed the following viscosity-temperature-pressure relationship.

$$H = S_o \Theta + Z_r \Pi + \log_{10} G_o$$

(3)

where

$$H = \log_{10} (\log_{10} \eta + 1.200)$$

$$\Theta = -\log_{10} (1 + T/135)$$

$$\Pi = \log_{10} (1 + p/2000)$$

$$G_o = \log_{10} (\eta_{o,0^\circ C} + 1.200)$$

The subscripts o, and r stand for atmospheric pressure and reference temperature. In the above equation, the units for viscosity, temperature and pressure are centipoise, Celsius and kgf/cm^2 respectively. The parameter S known as the 'Slope Index' is numerically equal to the slope of the viscosity-temperature line plotted on a rectifying chart (H vs. Θ) and Z, the 'Pressure Index' is the slope of the viscosity-pressure line plotted on a rectifying chart (H vs. Π). The other parameter G_o can be considered to be indicative of the viscosity grade of the oil, expressed in terms of dynamic viscosity. Roelands (1966) also determined that, for mineral oils for a wide range of viscosity values, the ratio $(Z_{40^\circ C}/S_o)$ remains fairly constant at 0.55. While Roeland's model is based upon absolute viscosity as a dependent parameter, fluidity (reciprocal absolute viscosity) is the preferred choice used in the THD analysis here and first introduced by Elrod (1991).
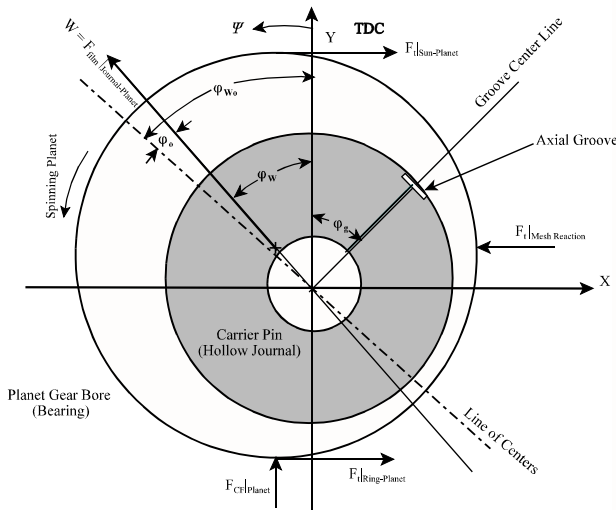

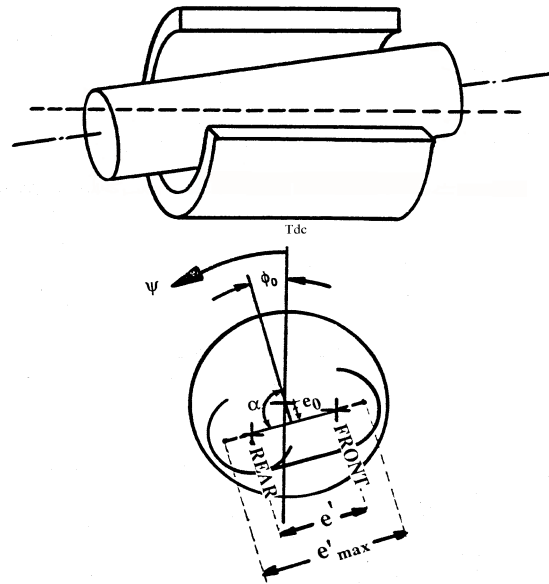**Figure 4 Force Diagram of the Bearing/Planet.**

Figure 5 Arrangement of Misaligned Journal Bearing.

The force diagram of the planet carrier configuration is shown in Figure 4 along with the defining position variables. The last term in the film thickness (Eqn. 4) is the contribution due to misalignment.

The film thickness is increased (decreased) by that amount linearly as one moves away from the axial center. With the aid of Figures 4 and 5, the film thickness can be written as

$$h = c + e_o \cos\left(\psi - \phi_{wo}\right) + e'_{max} \, D_m\left(y / L\right) \cos\left(\psi - \phi_{wo} - \alpha\right) \tag{4}$$

where

$D_m = e' / e'_{max}$

$\phi_{wo} = \phi_w + \phi_o$

$e'_{max} = 2 \left\{(1 - e_o^2 \sin^2\alpha)^{1/2} - e_o \left|\cos \alpha\right|\right\}$

Under general misalignment conditions, parameters' D_m, the degree of misalignment, and α, the angle between the projected journal rear center line and eccentricity vector at the center, defines the misalignment (refer to Fig. 5). e_o and ϕ_o represent the components to the eccentricity vector at the bearing axial center, ψ is the angular coordinate from the top-dead-center (TDC), ϕ_{wo} is the angle between the maximum film thickness and TDC, ϕ_w being the angle of the load vector from TDC, ϕ_o is the attitude angle between the load vector and the line of centers, e' is the value of the misaligned eccentricity determined from the projection of the complete journal onto the mid plane and e'_{max} is the maximum possible value. Note that as D_m approaches 1, the journal is touching the edge of the bearing and the misalignment is a maximum; for $D_m = 0$, the bearing and journal are perfectly aligned.

The Fourier heat conduction equation for the stationary journal, in cylindrical coordinates and in non-dimensional form, is written as

$$\frac{\partial \overline{T}}{\partial \tau} = \left(\frac{1}{P\,e_s}\right)\left[\frac{\partial^{\,2}\overline{T}}{\partial \overline{r}^2} + \frac{1}{\overline{r}}\frac{\partial \overline{T}}{\partial \overline{r}} + \frac{1}{\overline{r}^2}\frac{\partial^{\,2}\overline{T}}{\partial \psi^2} + \frac{\partial^{\,2}\overline{T}}{\partial Y^2}\right] \tag{5}$$

Equation (5) is applicable for the bearing/planet also, except that the circumferential temperature gradient term is assumed negligible based on the experimental investigation of Dowson, et al (1966-67) and that of Mitsui (1987). In those studies, the rotating element (shaft) surface temperatures were shown

to be nearly constant and could be essentially treated as isothermal for steady-state conditions. In this case, since the bearing/planet is rotating and the shaft is stationary, the inference can be made that the surface temperatures around the bearing housing are isothermal. Hence, the bearing temperature distribution is considered to be independent of the circumferential direction (ψ). However, the temperature variations in the axial and radial directions are still considered.

The cavitation boundary conditions are built-in Eq. (1). The thermal interface conditions to be imposed for film reformation and rupture boundaries and the treatment for any reverse flow in the film side of the reformation front is discussed in Elrod and Vijayaraghavan (1995). At the bearing-fluid interface, the thermal boundary conditions require continuity of temperature and heat flux, i.e.,

$$
\left.\overline{T}\right]_{\zeta=1} = \left.\overline{T}\right]_{\overline{r}=\overline{rbi}}
$$

$$
\frac{K_f}{2\pi} \int_0^{2\pi} \left.\theta_T \frac{\partial \overline{T}}{\partial \zeta}\right]_{\zeta=1} d\psi = \left. -K_b \frac{\partial \overline{T}_b}{\partial \overline{r}}\right]_{\overline{r}=\overline{rbi}} \tag{6}
$$

$$
\theta = \begin{cases} 1 \; if \; \theta \geq 1 \\ \theta \; if \; \theta < 1 \end{cases}
$$

Here, since the bearing is rotating, the net average heat flux of the fluid at the interface is matched with the bearing radial heat flux [Khonsari (1987), Vijayaraghavan (1996)]. The parameter, θ_T, is introduced here because, in the cavitated region, the film striations occupy only partial width and the heat from the film can be transferred to the metal only through this striation width. At the fluid-journal interface

$$
\left.\overline{T}\right]_{\zeta=1} = \left.\overline{T}\right]_{\overline{r}=\overline{rj}}
$$

$$
K_f \left(\theta_T \frac{\partial \overline{T}}{\partial \zeta} \right]_{\zeta=-1} = -K_j \left(\theta_T \frac{\partial \overline{T}}{\partial \overline{r}} \right]_{\overline{r}=\overline{rj}} \tag{7}
$$

At the outer and lateral end surfaces of the bearing shell, heat is transferred to the ambient through free convection, as defined by,

$$
\left(\frac{\partial \overline{T_b}}{\partial \overline{r}} \right)_{\overline{r}=\overline{rbo}} = -N\, u_b \left[\overline{T}_b \Big|_{\overline{r}=\overline{rbo}} - \overline{T}_a \right]
$$

$$
\left(\frac{\partial \overline{T_b}}{\partial Y} \right)_{Y=0,1} = -N\, u_b \left[\overline{T}_b \Big|_{Y=0,1} - \overline{T}_a \right]
$$

$$
\left(\frac{\partial \overline{T_j}}{\partial Y} \right)_{Y=0,1} = -N\, u_b \left[\overline{T}_j \Big|_{Y=0,1} - \overline{T}_a \right]
$$

(8)

The mixing temperature, $\overline{T}_m$, of the lubricant in the region of the groove can be determined by a simple heat balance in which the cooler supply lubricant mixes with the hot oil carry over fluid, i.e.

$$
\overline{T}_m = \frac{Q_h \overline{T}_h + Q_s \overline{T}_s}{Q_m}
$$

(9)

The subscripts, h, s, and m, indicate hot oil carry over, supply and mixture, respectively. Only the hot oil flowing at the groove axial locations are assumed to mix with the supply oil. The fluid and journal at the groove locations are considered to be at the mixture temperature.

When the applied forces on the bearing are specified (commonly known as the inverse problem) assumptions on eccentricity and attitude angle have to be made to start the computation. When the resulting fluid film forces are not of equal magnitude to the applied forces, the assumptions are revised using the following equations of motion,

$$M \frac{d^2 e_x}{dt^2} = W_x - F_x$$

$$M \frac{d^2 e_y}{dt^2} = W_y - F_y$$

(10)

where

$$W_x = -\int_0^{2\pi} \int_{-L/2}^{L/2} p \cos(\psi) R \, d\psi \, dy$$

$$W_y = \int_0^{2\pi} \int_{-L/2}^{L/2} p \sin(\psi) R \, d\psi \, dy$$

$$e_o = \left(e_x^2 + e_y^2 \right)^{1/2}$$

$$\phi_o = \tan^{-1}\left(\frac{e_x}{e_y} \right) - \phi_w$$

e_x and e_y are the eccentricities in the vertical and horizontal directions respectively. At steady state, it is desired that the forces match and the velocity and the acceleration of the journal center vanish.

SOLUTION PROCEDURE

The numerical procedure in solving the above equations has been described by Vijayaraghavan (1996). Once the number of internal Lobatto points is chosen, their location and corresponding Legendre polynomials can be determined. The Legendre coefficients for fluidity, velocity, flow, and temperature gradients are computed and stored as matrices. For a given misalignment condition and applied radial and tangential forces, initially the eccentricity ratio and attitude angle are assumed. Fluidity values are determined at all points based on the latest available temperature and pressure values. Effective fluidity (ξ_p) is determined and the hydrodynamic equation (Eq. 1) is solved using a cavitation algorithm. From the total mass flow rates across the film thickness, point wise velocity, flow, flow gradients and dissipation can be determined. Then the energy equation is solved to determine the

temperature distribution in the fluid. A suitable number of Lobatto points are also chosen for journal and bearing shell metal domains in the radial direction and their temperature gradients are also expressed in terms of Legendre polynomial. The entire system is solved simultaneously to determine the temperature distribution.

The thermal boundary conditions at the fluid-solid interfaces (Eqns. 6-8) are expressed in terms of all the internal Lobatto point temperatures. After the temperature distribution is determined for internal points, the boundary temperatures are determined, satisfying the respective boundary conditions. At each time step, the switch function (g) values in Eq.(1), and the boundary temperatures are updated. The fluid mixture temperature at the groove is also determined at each time step, based on the total flow and the averaged fluid temperature for the groove width at the groove inlet and the side leakage rate. It is assumed that, the journal-fluid interface is at supply temperature, bearing-fluid interface is at mixture temperature and at internal Lobatto points, the temperature is determined based on the ratio of flow rate. However, all nodes in the groove are assumed to be at the supply pressure. Inside the surface of the hollow journal, through which the lubricant is supplied, is assumed to be at the constant supply temperature. Based on the new temperature and pressure distribution, revised fluidity values are determined and the procedure is repeated until the θ and $\bar{T}$ values at all nodes and points, between two iterations are within a set limit.

After the steady state conditions are achieved, the load capacity and the attitude angle are determined from the pressure distribution. If the calculated fluid film forces differ from the applied forces by a preset accuracy and/or the calculated attitude angle is different from the previously assumed value by more than the required accuracy, equations of motion (Eq. 10) are solved to update the assumption on the eccentricity ratio and attitude angle and the procedure is repeated, until the required accuracy is achieved.

The hydrodynamic equation is solved using a cavitation algorithm by Douglas and Gunn (1964), suitably modified for the present equation, using an alternating-direction-implicit (ADI) method, to determine the updated θ distribution. Mass and energy conservation across the cavitation interfaces are

rigorously implemented. The fluid energy and solid conduction equations are simultaneously solved using a 3D-ADI method by Douglas and Gunn (1964, 1984), to determine the temperature distribution at all internal Lobatto points. The equations of motion (Eq. 10) are solved using the 4th order Runge-Kutta method.

All the governing equations are in the transient form. Although, in the present case, only the steady state values are of interest. The time derivatives serve as a source of numerical dissipation and the time steps can be used as a control parameter to achieve stable and faster convergence toward the steady state. In order to speed up the computation to determine the asymptotic steady state temperature distribution, a dual time step procedure is used (i.e.., a larger time step for the metal conduction and a smaller time step for the fluid film). Paranjpe and Han (1994?) also determined that the time scale for thermal transients of the journal and bearing shell are about 3 to 4 orders of magnitude higher than those for the fluid. The steady state results are found to be essentially independent of the time steps used.

The planetary gear journal bearing considered in this study is an axially grooved, finite, rigid, circular bearing. The rotating bearing shell is assumed to be made of bronze-lead and the hollow journal is made of steel. Supply lubricant flows through the journal bore, exiting at the groove. The groove is of a 30° angular extent, extends only up to half of the bearing length with its center line located at 45° from top dead center (tdc) of the bearing. The load angle, depending upon the applied forces, varies from 0° to 45° from tdc. The bearing parameters used for this study are shown in Table I. For the bearing considered, 3 internal Lobatto points across the film thickness, 3 across the bearing shell thickness and 5 across the journal radius are used. A total of 49 nodes around the circumference and 15-19 nodes evenly distributed over the bearing length is used for smaller misalignments. If the degree of misalignment is more than 0.7, 25 nodes in the axial direction are used, some of them strategically located near the maximum pressure location. The convergence accuracy of 10^{-6} for θ, 10^{-3} for T, 0.1% for forces and 0.1^o for ϕ_o are applied. The code is run on a Cray YMP super computer for all the cases. Typically, the CPU time required for a case ranges from 200 - 600 seconds.
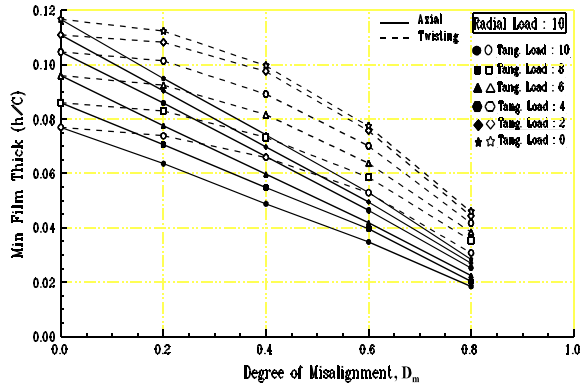
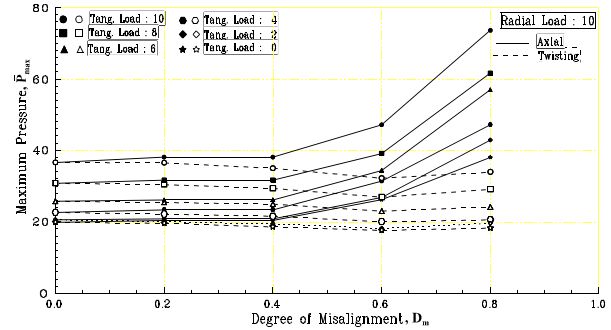**Figure 6 Effect of Misalignment on Minimum Film Thickness.**

Figure 7 Effect of Misalignment on Maximum Pressure

RESULTS AND DISCUSSION

The planet gear considered in this study rotates around the carrier pin and also revolves around the sun gear at a constant speed, irrespective of the torque load being transmitted (refer Fig. 1). Hence, the non-dimensional radial load on the bearing is assumed to be constant at 10. The non-dimensional tangential load on the bearing, a measure of the torque load being transmitted, varies from 0 to 10. The misalignment is assumed either to be axial ($\alpha=180^o$) or twisting ($\alpha=90^o$). The general misalignment effects can be deduced from these limiting cases. The degree of misalignment, D_m is varied from 0. to 0.8. Steady state solutions are achieved when the fluid film forces match the applied forces in magnitude and the assumed attitude angle matches the computed value. This study is performed with non-dimensional parameters, to provide some generality for the results to be interpreted for various combinations of bearing data and operating parameters.

Figure 6 indicates the non-dimensional minimum film thickness variations, $\overline{h}$, with respect to the degree of misalignment, D_m, for various tangential load values, $\overline{F}_t$. Increasing the degree of misalignment causes a decrease in minimum film thickness for either axial or twisting misalignment. The effect on bearing performance becomes a critical consideration at high D_m, more so for axial

15

misalignment than for twisting misalignment   With axial misalignment, the minimum film thickness is almost 4 times smaller at $D_m = 0.8$, compared to an aligned bearing. By comparison, the minimum film thickness resulting from twisting misalignment is 2.6 times smaller at $D_m = 0.8$. In general, the minimum film thickness is less sensitive to increases in D_m for misalignment caused by twisting, especially in the range $D_m \leq 0.4$. The plots obviously approach zero at maximum possible misalignment. The non-dimensional maximum pressure, $\overline{p}_{max}$, in Fig.. 7, shows little or no change to increases in misalignment for small misalignment, i.e., in the range $D_m \leq 0.4$. With axial misalignment, the maximum pressure dramatically increases above this range, almost doubling at $D_m=0.8$. There is no significant change in maximum pressure with twisting misalignment and in fact, the value slightly reduces with increase in misalignment. As expected, the maximum pressure location is off the axial center of the bearing. DuBois et al (5) and Vijayaraghavan and Keith (9) have
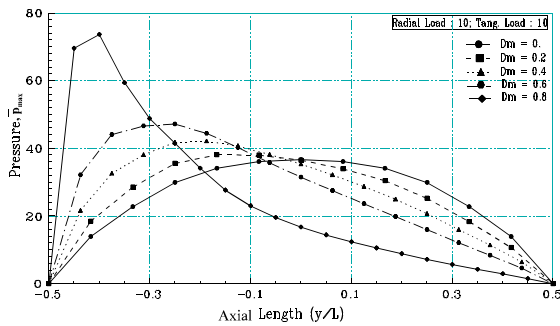

Figure 8 (a) Axial Pressure Profile for Axial Misalignment (at Maximum Pressure Location).
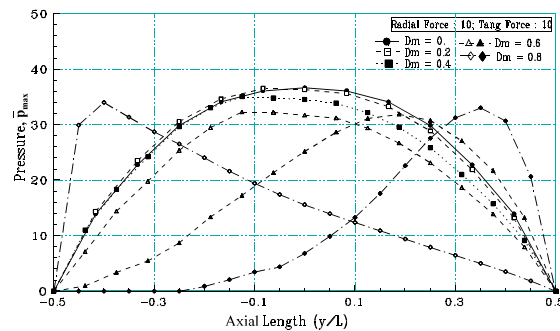

Figure 8 (b) Axial Pressure Profile for Twisting Misalignment (at Maximum Pressure Location).

shown such a shift with three-dimensional pressure profile plots for misaligned bearings. With axial misalignment (Fig. 8 (a)) the maximum pressure region moves toward one edge of the bearing as the misalignment increases. In the case of twisting misalignment (Fig. 8 (b)), although the maximum pressure value does not increase, there are two peak pressure humps moving toward both edges of the bearing with a phase lag in the circumferential direction.
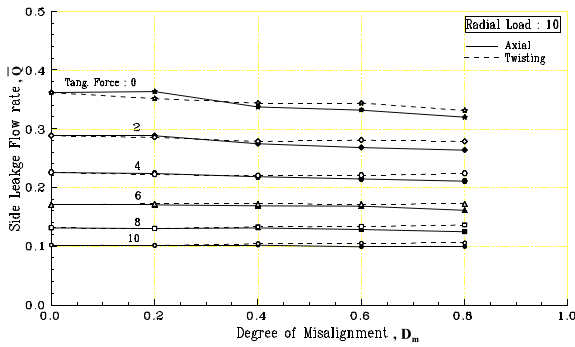
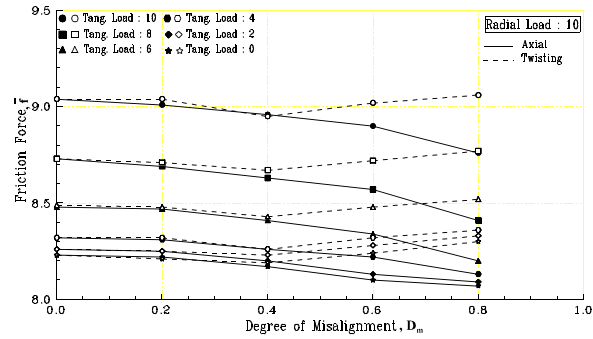**Figure 9 Effect of Misalignment on Side Leakage**

Figure 10 Effect of Misalignment on Friction Force

As can be observed from Figs.9 and 10, the side leakage rate and the friction force (power loss) are not significantly affected by misalignment. It is interesting to note from Fig. 9 that, the side leakage rate for higher torque load transmitted is considerably lower than for lower transmitted loads. This is because with higher tangential load, the load vector (Fig. 4) moves farther away from the groove. Hence, the film thickness at the groove is lesser and with a smaller active film region, the leakage rates are lower. However, the power loss increases with the load.

Figure 11 quantifies the variation in non-dimensional maximum fluid temperature at various tangential loads due to misalignment. The temperature rise is almost linear at lower degrees of misalignments and exponentially increases for $D_m > 0.4$. The temperature rise is more pronounced for an axial misalignment, by about 10% for $D_m = 0.4$ and about 30% for a misalignment of 0.8,

compared to an aligned bearing. With twisting misalignment, there is only a marginal temperature rise, by about 5% even for $D_m = 0.8$. This pattern goes in line with the corresponding rates of variation in minimum film thickness and maximum pressure for these types of misalignments. In most cases, the maximum fluid temperature occurs at the journal surface,
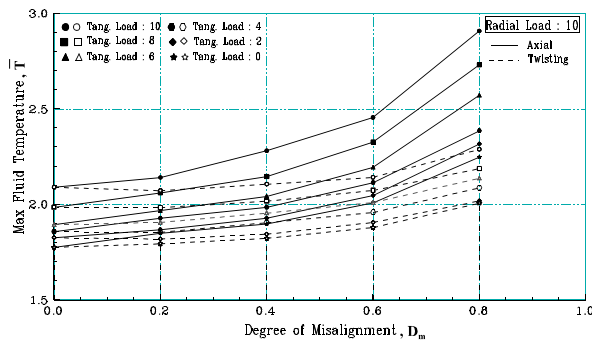

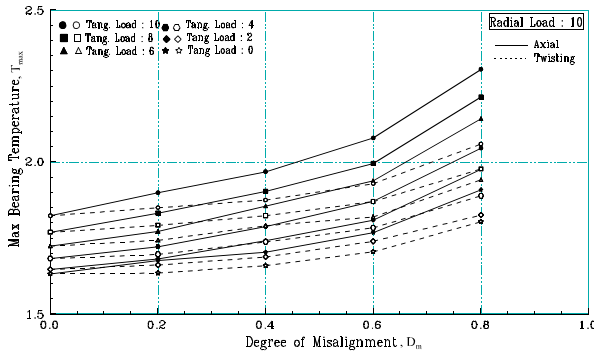**Figure 11 Effect of Misalignment on Maximum Fluid Temperature**

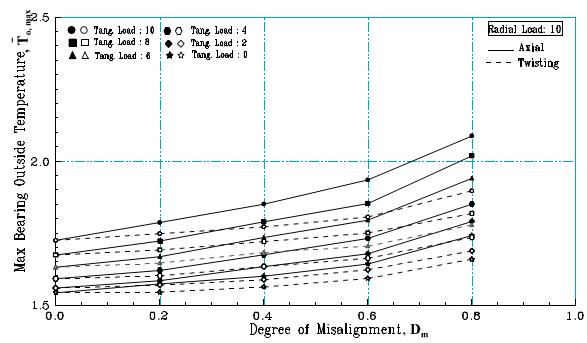**Figure 12 Effect of Misalignment on Maximum Bearing Temperature, $\overline{T}_{max}$**

Figure 13 Effect of Misalignment on Maximum Outside Surface Temperature, $\overline{T}_{o,\,max}$.

near the minimum film thickness region. Axially, the maximum fluid temperature occurs near the axial end of the bearing, where the film thickness is smaller and where the width of the groove does not extend to, resulting in no direct mixing of the hot oil with the cooler supply lubricant.

Variations in non-dimensional maximum bearing temperature at inside and outside surfaces are shown in Figs. 12 and 13. The trend in temperature rise is similar to the film temperature variation. The rate of temperature rise is almost linear up to D_m=0.6 and nonlinear beyond. With large axial misalignments, the bearing temperature can increase by about 30% when compared to an aligned bearing at the same load. It should be noted that, since the bearing is rotating, the temperature flux at the fluid-bearing interface is averaged and the temperature is independent of the circumferential direction.

Because of the axial variations in film thickness profile and asymmetry in pressure profile due to misalignment, there exists a considerable variation in axial temperature profile too. Figure 14 indicates the axial variation of the circumferentially averaged bearing outside surface temperature, when the applied non-dimensional radial load is 10 and tangential load is 10. With axial misalignment, there is a considerable variation along the bearing length, as much as 0.25-0.5, larger variation being at higher misalignments. With the twisting misalignment, the axial variations are less pronounced, but the temperature levels are generally higher than those at an aligned condition. There
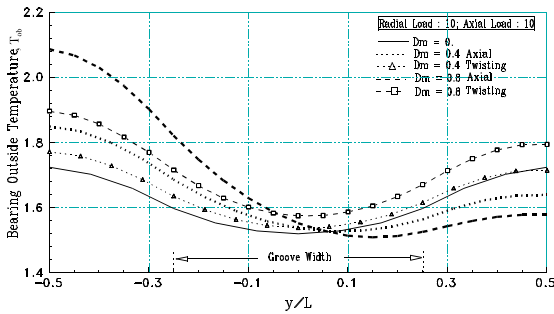
18

Figure 14 Axial Variation of Bearing Outside Temperature for $\overline{F}_t = 10$.
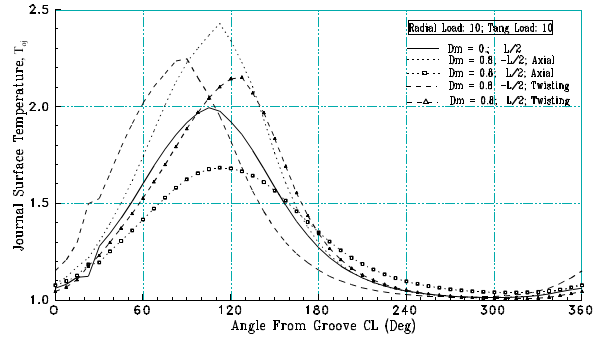
Figure 15 Circumferential Journal Surface Temperature for $\overline{F}_t = 10$.

is a dip in the temperature profile around the axial center of the bearing because of the presence of groove, which supplies cooler lubricant. The cooler supply mixes with the incoming hot oil carry over within the groove width, resulting in lower temperature levels. As can be seen from these figures, the temperature dip is more pronounced with no tangential load because the supply rate is larger. The temperature profile for an aligned bearing is also shown in these figures for the ease of comparison.

The stationary journal has a three-dimensional temperature profile. Figure 15 is the journal outer surface temperature around the circumference at both bearing edges, at D_m=0.8 and for a tangential load of 10. With axial misalignment, the temperature peaks at either end are quite different, but occur at the same circumferential location. Whereas with twisting misalignment, the temperature peaks at both ends are similar in magnitude, but occur at different circumferential locations. Notice that the temperature drops quite rapidly from the peak, which occurs about the film rupture location and in the cavitated region, the temperatures are closer to the supply temperature. The slight wiggles in the temperature profile near the groove exit, particularly at higher loads, is due to the reverse flow occurring near the stationary journal, due to adverse pressure gradient at the film reformation. As shown by Elrod and Vijayaraghavan (1995), this numerical procedure, even with just three internal Lobatto points, is sensitive enough to bring out this effect.

19

D. Vijayaraghavan
and D. E. Brewe

CONCLUSIONS

Misalignments in planetary gear journal bearings are a very real operating problem and understanding the effects of such misalignment on the performance of the bearing is very important. In this report, the journal bearing of a planet gear of an epicyclic gear train is analyzed for misalignment effects. Different values of torque load transmitted, with a constant radial load due to the carrier rotation around the sun gear, are considered. A comprehensive THD analysis is applied that includes viscosity variation through the film, heat transfer from the fluid to the metal and heat conduction through the journal and bearing. However, it excludes differential thermal expansion/contraction of the shaft and housing which was noted earlier could have an effect on the accuracy of results but not to the extent that it would affect the conclusions drawn. The model includes the Elrod algorithm, rigorously implementing conservation of mass flow and energy through the entire bearing clearance. Purely axial or twisting misalignments are considered in this analysis. Although, the alignment can be in any arbitrary direction, the effects on performance can be easily assessed by knowing the individual effects. The variables are non-dimensionalized to provide some degree of generality to the results. For the cases studied, the following are the major conclusions:

1. Axial misalignments have much more devastating effects on minimum film thickness, maximum pressure and temperatures of fluid and metal than twisting misalignments.

2. With degree of misalignment less than 0.5, there is no significant effect.

3. For axial misalignment with D_m=0.8, the minimum film thickness reduces by four times, peak pressure doubles and temperatures increase by about 30%, compared to an aligned bearing at the same load. At higher misalignments the variations are nonlinear and much more pronounced.

4. For twisting misalignment the variations are less severe. With D_m=0.8, the minimum film thickness halves, peak pressure remains almost the same and temperatures increase by about 5%, compared to an aligned bearing at the same load. At higher misalignments the rate of variation is more pronounced, but not as severe as axial misalignment.

5.   Side leakage rate and power loss do not significantly change due to misalignment.

6.   Non-symmetrical pressure and temperature variation along the axial length of the bearing becomes progressively more pronounced as the misalignment increases.

NOMENCLATURE

c - Radial clearance

c_p - Specific heat

D - Journal diameter

D_m - Degree of misalignment

e - Eccentricity

F - Applied forces

H - Viscosity parameter

h - Film thickness

h_t - Heat transfer coefficient

K - Thermal conductivity

L - Bearing length

M - Mass equivalent of the bearing/planet

P_L - Power loss

p - Fluid pressure

Q - Flow

R - Journal radius

r - Radius

S - Slope Index

T - Temperature

t - Time

U_L - Non zero surface velocity

u - Fluid velocity in x direction

$\overline{V}$ - Velocity vector ($u\overline{e}_x + v\overline{e}_y$)

v - Fluid velocity in y direction

W - Load capacity

x - Circumferential coordinate

y - Axial coordinate

Z - Pressure Index

z - Coordinate across film thickness

α - Misalignment angle

β - Bulk modulus

ε - Eccentricity ratio

Φ - Viscous dissipation

ϕ - Attitude angle

η - Viscosity

κ - Diffusivity

Π - Pressure parameter

Θ - Temperature parameter

ρ - Fluid density

ω - Angular velocity

ξ - Fluidity ($1/\eta$)

ξ - Legendre coefficient

ψ - Angular coordinate from groove CL

Subscripts

a - ambient

b - bearing

c - cavitated region

CF - centrifugal force

f - film

g - groove

j - journal

L - lower wall ($\varsigma = -1$)

R - reference

s - supply

U - upper wall ($\varsigma = +1$)

23

Non-dimensional Parameters

$\overline{h}$ - h/c

Nu – $h_t R/K$

Pe_f – $cU_L/\kappa\,(c/R)$

Pe_s – $U_L R/\kappa$

$\overline{p}$ - $(p/\omega_L\eta_R)\,(c/R)^2$

$\overline{P}_L$ - $(P_L/\omega_L\eta_R L)\,(c/R)$

$\overline{Q}$ - $Q/cwRL$

$\overline{r}$ - r/R

$\overline{T}$ - T/T_R

$\overline{u}$ - u/U_L

$\overline{v}$ - v/U_L

$\overline{V}$ - V/U_L

$\overline{W}$ - $(W/\omega_L\eta_R RL)\,(c/R)^2$

Y - y/R

$\overline{\beta}$ - $(\beta/\omega_L\eta_R)\,(c/R)^2$

ε - e/c

Φ^* - $(\rho c_p T_R/\omega_L\eta_R)\,(c/R)^2$

τ - $\omega_L t$

$\overline{\xi}$ - ξ/ξ_R

ψ - x/R

ζ - $z/(h/2)$

REFERENCES

Anderson, D. A., Tennehill, J. C. and Pletcher, R. H. (1984). *Computational Fluid Mechanics and Heat Transfer*, **Hemisphere Publishing Corp.**, New York, pp 99-117.

Braun, M. J., Mullen, R. L. and Hendricks, R. J. (1983). "An Analysis of Temperature Effects in a Finite Journal Bearing with Spatial Tilt and Viscous Dissipation", **ASLE Transactions**, Vol 27, No 4, pp 405-412.

Das, P. K. and Gupta, S. S. (1980). "An Analytical Method to Calculate Misalignment in the Journal Bearing of a Planetary Gear System", **Wear**, Vol 61, pp 143-156.

Douglas, J. and Gunn, J. E. (1964). "A General Formulation of Alternating Direction Methods- Part I: Parabolic and Hyperbolic Problems", **Numerische Mathematik**, Vol 6, pp 428-453.

Dowson, D., Hudson, J., Hunter, B. and March, C. (1966-67). "An Experimental Investigation of the Thermal Equilibrium of Steadily Loaded Journal Bearings", **Proc. Inst. of Mech. Engr**., Vol 101, Part 3B, pp 70-80.

DuBois, G. B., Ocvirk, F. W., and Wehe, R. L. (1951). "Experimental Investigation of Oil Film Pressure Distribution for Misaligned Plain Bearings", **NACA TN-2507**.

DuBois, G. B., Ocvirk, F. W., and Wehe, R. L. (1957). "Properties of Misaligned Journal Bearings", **Transactions of ASME**, Vol 79, pp 1205-1212.

Elrod, H. G (1991). "Efficient Numerical Method for Computation of Thermohydrodynamics of Laminar Lubricating Films", **ASME Journal of Tribology**, Vol 113, pp 506-511.

Elrod, H. G. and Vijayaraghavan, D. (1995). "Film Temperatures in the Presence of Cavitation", **NASA CR - 195481. US Army ARL - CR - 231**.

Khonsari, M. M. (1987, "A Review of Thermal Effects in Hydrodynamic Bearings: Part I-Slider and Thrust Bearings; Part II-Journal Bearings", **ASLE Transactions**, Vol 30, pp 19-33.

Lynwander, P. (1983). *Gear Drive Systems: Design and Application*, Published by **Marcel Dekker Inc**.

McKee, S. A. and McKee, T. R. (1932). "Pressure Distribution in the Oil Film of Journal Bearings" **Transactions of ASME**, Vol 54, pp 149-165.

Mitsui, J. (1987). "A Study of Thermohydrodynamic Lubrication in a Circular Journal Bearing," **Tribology International,** Vol. 20, No. 6, pp 331 - 341.

Paranjpe, R. S. and Han, T. (1994). "A Transient Thermohydrodynamic Analysis Including Mass Conserving Cavitation for Dynamically Loaded Journal Bearings", Presented at **ASME/ STLE Tribology Conference**, Maui, Hawaii, Paper: 94-Trib-36.

Pinkus, O. and Bupara, S. S. (1979). "Analysis of Misaligned Grooved Journal Bearings", ASME Journal of Lubrication Technology, Vol 101, pp 503-509.

Pinkus, O. (1990). *Thermal Effects in Fluid Film Tribology*, **ASME Press**, New York.

Roelands, C. J. A. (1966). Correlational Aspects of the Viscosity-Temperature-Pressure Relationship of Lubricating Oils, PhD Thesis, Univ. of Delft, Netherlands, O.P., Books Program, **University Microfilms**, Ann Arbor, MI.

Smalley, A. J. and McCallion, H. (1966). "The Effect of Journal Misalignment on the Performance of a Journal Bearing Under Steady Running Conditions", **Proceedings of the Institution of Mechanical Engineers**, Vol 181(3B).

Vijayaraghavan, D. and Keith, Jr., T. G. (1990). "Analysis of a Finite Grooved Misaligned Journal Bearing Considering Cavitation and Starvation Effects", **ASME Journal of Tribology**, Vol 112, No 1, pp 60-67.

Vijayaraghavan, D. and Keith, T. G. Jr. (1989). "Development and Evaluation of a Cavitation Algorithm", **Tribology Transactions**, Vol 32, No.2, pp 225-233.

Vijayaraghavan, D. (1996). "An Efficient Numerical Procedure for Thermohydrodynamic Analysis of Cavitating Films", **ASME Journal of Tribology**, Vol 118, No.3, pp 555-563, NASA CR - 195476.

TABLE I: Bearing and Operating Parameters

$L/D = 1.33$	$\beta = 400$
$c/R = 0.0017$	$Pe_f = 40$
$R_{bo}/R_{bi} = 1.67$	$Pe_b = 6.5 \times 10^4$
$R_{ji}/R_{jo} = 0.33$	$Pe_j = 8.0 \times 10^4$
$\psi_g = 30^\circ$	$Nu_b = 0.05$
$L_g/L = 0.5$	$\Phi * = 45$
$\phi_g = 45^\circ$	$K_j/K_f = 250$
$\overline{p}_s = 0.10$ (40 psi)	$K_b/K_f = 425$
$\overline{p}_c = 0.$	$\overline{T}_a = 1.0$
$\overline{p}_a = 0.$	$D_m = 0$ to 0.8
$\overline{T}_s = 1.0$	$\alpha = 180^\circ, 90^\circ$
$\eta_R = 0.36$ Pa S	$S = 1.0$
$T_R = 60 \,^\circ C$	$Z = 0.55$